ELSEVIER

Materials Science and Engineering A 472 (2008) 15–25

MATERIALS SCIENCE & ENGINEERING A

www.elsevier.com/locate/msea

Aluminium AA2024 T351 aeronautical alloy Part 1. Microbial influenced corrosion analysis

Blanca M. Rosales [a,*,1], Mariano Iannuzzi [b]

[a] *CIDEPINT, Av. 52 s/n, 121 y 122 B1900AYB, La Plata, Argentina*
[b] *Department of Materials Science and Engineering, Ohio State University, USA*

Received 26 January 2006; received in revised form 28 January 2007; accepted 28 June 2007

Abstract

The aim of this paper was to correlate the elemental distribution of alloying elements with the MIC attack morphology of the AA2024 T351 alloy by the fungus *Hormoconis resinae*. Anodic polarisation was applied up to the E_p of the AA22024 alloy after different thermal treatments, especially T351, and to Al 99.999% as reference. The aqueous solutions were sterile Bushnell–Haas culture medium employed both as mineral nutrient for fungal growth and as support electrolyte. The variation in aggressiveness of cultures with time was also electrochemically analysed. The attack after different tests was evaluated using ESEM, SEM, EDX and optical microscopy. It was demonstrated the MIC susceptibility of the AA2024 T351 alloy to fungal cultures and the dangerous tunnelling morphology of the respective attack through grain boundaries.

Keywords: Aluminium AA2024 T351 alloy; Microbiological influenced corrosion; Aeronautical applications; Service condition risks

1. Introduction

The necessity of increasing flight autonomy of both commercial and military aircraft led designers to use structural parts of aircraft as fuel storage deposits. All those components have intricate designs hindering fluid circulation and easy maintenance.

Dissolved traces of water used in oil process remain dissolved in the fuel. During flight the structure cools down decreasing water solubility in fuel and provoking its accumulation at the wing bottom by density difference. The presence of separate water sets up as an essential condition for microorganism growth and should be daily eliminated through drainage valves.

Since the first days of aviation there have been reports of damage caused by microorganisms. The first wooden propellers and tarpaulin canvas components in general underwent attack of diverse fungal species.

The problem of biological contamination increased when kerosene became the propellant of turbines in replace of gasoline, being even emphasised when wings begun to be used as integral tanks. These changes occurred first in military aviation (around the 1950s) and later in commercial aircraft (the 1960s) because the Jet A1 or JP1 kerosene used as the new fuel was a better carbon source for microbes.

Biologic sludge of fuel tanks is composed of around 40 species of bacteria, yeast and filamentous fungi. Although at first associated to bacteria only, it was soon found that a fungus (then designed *Amorphoteca resinae*, *Cladosporium resinae* [1]) and later *Hormoconis resinae*, was always present.

It is known that microorganisms cannot grow in the absence of liquid water and that corrosion problems in contaminated aircraft fuel tanks is caused by microbial action. Thus that tank water drainage is a mandatory operation in turbine-propelled aircraft. Even when this prescription alone is far from solving the problem it contributes to diminish proliferation risks.

Although contamination of fuel tanks is one of the most severe problems detected in the aviation industry [2], its incidence in commercial aviation was since its beginning far lower than in military aircraft.

In 1971 Scott [3] observed the correlation existing between microbial contamination, climate and aircraft flight conditions. He found that the problem was much more frequent and severe in hot and humid regions or in tropical or subtropical climates. In this way it was possible to define what is today known as *areas of high or low* contamination risk [4].

* Corresponding author. Tel.: +54 11 4782 9921; fax: +54 11 4782 9921.
E-mail addresses: brosales@fibertel.com.ar (B.M. Rosales), iannuzzi.1@osu.edu (M. Iannuzzi).
[1] Researcher of the Consejo de Investigaciones Científicas y Técnicas (CONICET).

0921-5093/$ – see front matter © 2007 Elsevier B.V. All rights reserved.
doi:10.1016/j.msea.2007.06.079

A great number of these events use to occur in aircraft remaining long periods on ground (military) or having low frequency utilisation (executive, private) due to microbial proliferation in their tanks. The most frequently referred problems are:

(1) Fuel filter clogging linked to the magnitude of biologic development and small pore size of filters. Such obstruction may be correlated to biologic sludge characteristics as texture, which in the case of the fungus *H. resinae* is tough, while bacterial sludge consists of fine particles dispersing by stirring [5,6]. There exists strong evidence that some fungi, especially *H. resinae* and certain bacteria as *Pseudomonas aeruginosa* [7] cause pitting corrosion in fuel tanks bottoms.
(2) Both water and sludge may affect the fuel quantity indicators, especially those of capacitive type, as well as other instruments and gauges of the fuel system. Erratic readings in the fuel quantity indicators may be the cause of serious accidents when there is not enough fuel left to reach an alternative airport.
(3) Microbial proliferation may deteriorate the fuel quality, something fundamental in modern jets, while in airplanes previous to the 1950s the fuel quality was not determinant in piston-powered aircraft efficiency [1].
(4) And lastly, what constituted the aim of our research work during past three decades, biologic sludge is in itself corrosive to the aeronautical aluminium alloys. This is a localised process diminishing the alloy thickness on the affected area even up to its drilling.

Being points of stress concentration, pits may in turn nucleate flaws. Thus, MIC on overloaded wing structures might cause catastrophic failures during flight.

1.1. Corrosion of pure aluminium

Aluminium and its alloys are extensively used in industry because they combine good physical properties, adequate mechanical performance and quite good resistance to uniform corrosion. However, they suffer localised attack in diverse corrosive media.

In spite of their electrochemical behaviour similar to other alloys undergoing pitting, its study is of particular interest, as pits do not show the typical hemispheric shape and polished bottom of other metals. Al pitting morphology in presence of Cl^- ions might lead to nucleation of not proper pitting. As Galvele and de De Micheli [8] have shown, anodic polarisation curves are characterised by a passivity zone where no attack is observed; however, surpassing a certain critical potential, the current drastically increases and pitting occurs. Besides it has been demonstrated that this critical potential does not depend on any induction time.

Morphology of attack observed during anodic polarisation in $NaNO_3$ solutions depends on the technique used for anodic potential scanning. Potentiostatic techniques reveal hemispheric pits, frequently covered by a poorly adhesive layer of corrosion products at the bottom, "dry sludge". Galvanostatic techniques, on the contrary, result in crystallographic pits.

As morphology of aluminium and its alloys pitting strongly depend of variable NaCl and KNO_3 mixtures this study was performed in the absence as compared to in the presence of fungal cultures as when NO_3^- from a sterile culture medium is consumed increasing the relative [Cl^-] during fungal growth. Transition was found in both cases between hemispheric to crystallographic pits.

1.2. Metallurgical state and chloride effect on the electrochemistry of Al 99.999%

Due to NO_3^- consumption as N source by the *H. resinae* fungus, the Al 99.999% electrochemical behaviour was analysed for different NaCl concentrations in KNO_3 0.1 M aqueous solutions. The electrochemical effect of the increase in the Cl^- aggressive ion to the NO_3^- passivating ion concentration rate was thus studied. Also the influence of the Al metallurgical condition was electrochemically and through surface analysis evaluated using samples in rolled and re-crystallised state.

1.3. AA2024 alloy metallographic and composition study through optical microscopy and SEM–EDX

The aim of the AA2024 T351 alloy study was the semi-quantitative verification of the presence and distribution of precipitates and secondary phases.

Specimens were polished from 600 grade paper to 3 μm diamond paste. The last polishing stages (to 3 μm) were made with extreme care as certain precipitates can be pulled out of the matrix producing profound scratches. Part of the samples were polished electrolytically with 90–10 solution (90% butyl cellozolbe, 10% perchloric acid) for further analysis without metallisation, using SEM–EDX, while another samples set was submitted to chemical etching using Keller's reagent and optical microscopy.

As the extraction bulk of the SEM beam is in the order of the cubic micron [9], composition analysis could only yield qualitative content and distribution of the phases. Nevertheless, this study aims at verifying the existence of such precipitates, besides their morphology and spatial disposition. These data are of the utmost importance at the time of approaching the phenomenology of alloy pitting and understanding the influence of each phase over said phenomenon. From analysis of the composition mapping we verified that Al–Cu–Mn–Fe precipitates are the largest in size and were found in higher proportion. Likewise, precipitates of Al–Cu and Al–Cu–Mg may be observed, their existence being confirmed through EDX in different areas of the samples tested. Their form is less geometrical than those of the Al–Cu–Mg–Fe precipitates (as also reported Blanc et al. [10]). Finally, Al–Cu–Fe precipitates were not found in significant proportion.

1.3.1. Electrochemical behaviour of the AA2024 alloy

As already seen, copper distribution in the AA2024 alloy is not homogeneous [11]. This fact, associated to inter-metallic particles in the material, originate galvanic cells, giving rise to localised attack, to phases of lower pitting potential than

that of the aluminium matrix. The importance of such precipitates, especially copper-containing ones, has also been studied in connection with the composition gradient around those phases, as initiators of different type of corrosion as intergranular and SCC. From E_c measurements of the several phases, it was confirmed that precipitates of Al–Cu–Mn–Fe (type 1) are nobler than the matrix, and do not contribute to localised attack, while precipitates Al–Cu–Mg (type 2) are more active.

At low potentials it was found that Cu dissolved from inter-metallic particles is re-deposited on the surface at sites dominating the corrosion process. Pitting nucleation rate is much higher than in pure Al in the zone of low potentials. Over high potentials, where there is no copper re-deposition, pit nucleation is much slower, and the behaviour is similar to that of pure Al.

De-alloying processes by preferential dissolution of Al and Mn might be responsible for Cu enrichment over the inter-metallic particles. However at E_c, simultaneous dissolution of both Al and Cu followed by copper reduction seems to be unlikely. Buchheit et al. [12] proposed a phase S de-alloying mechanism (Al_2CuMg) which might result in porous small copper particles formation on the alloy surface.

The distribution and size of certain precipitates, as well as the composition gradient around them could influence failure mechanisms, such as inter-granular corrosion, MIC and stress corrosion cracking (SCC), of great importance in aircraft fuel tank integrity.

1.3.2. Influence of thermal treatment on the AA2024 alloy electrochemical behaviour

To achieve better understanding on AA2024 electrochemical behaviour anodic polarisation tests were carried out on samples with different thermal treatments.

The interest in the AA2024 T351 alloy excellent mechanical properties is the cause for to its use as the lower skin of aircraft integral fuel tank, where however, MIC and SCC may occur.

The purpose of this paper is to determine the effect of alloying element surface distribution and of the environmental composition on the alloy susceptibility to MIC attack by the fungus *H. resinae*.

2. Experimental

2.1. Reference metal: high purity aluminium

Cold rolled 30% deformation and re-crystallised Al 99.999% samples were polished up to 0.25 μm diamond paste. Due to the low temperature of Al re-crystallisation and very high purity of the material, care was taken to avoid heating of samples at any stage of the preparation process.

Coupons of 20 mm × 10 mm were cut from 1 mm thick sheets of the 2024 T351 alloy and from Al 99.999% and it was verified that second phases were not eliminated during the alloy polishing. Due to anisotropy of the alloy respect to its anodic behaviour all samples were tested in L-T direction, coincident with the exposed flat inner surface of aircraft fuel tank.

Table 1
Thermal treatments performed to the AA2024 alloy

Temperature (°C)	Time (h)	Designation (aluminium association)
25	72	T4
190	3	–
190	22	–
190	27	T7

2.2. Thermal treatments on the AA2024 alloy

The thermal treatment consisted on the 2024 alloy solubilisation at 495 ± 6 °C during 35 min. This is a very critical temperature because overheating would produce the alloy burning. This is that a liquid phase appears at grain boundaries caused by an euthectic at 501 °C irreversibly deteriorating all the alloy properties. Once reached the above-mentioned time the samples were rapidly quenched in water at 20 °C. After 5 s since the door oven opening to the total samples immersion the θ phase precipitation occurs. Also, the water temperature must not increase more than 18 °C. A k-type thermocouple was used on the alloy to carefully control the very critical temperature condition of the previous operation [13].

Then, the natural ageing during different times (3, 22, 27 and 72 h) was applied as summarised in Table 1. Once finished, the evolution with time of the Brinell hardness was determined as a function of the ageing time and the results were verified by comparison with the respective curves in the Metal Handbook [13]. Final microstructures were obtained on the alloy samples.

As thermal treatment determines the mechanical and corrosion resistance of an alloy this aspect of the work was approached to demonstrate the relationship between the metallurgical structure and its electrochemical behaviour in microbial cultures. Thus, the different structures may be classified to select the one minimising the risks under study.

2.3. Microbial cultures

A strain of the *H. resinae* fungus was seeded in modified Bushnell–Hass (B–H) mineral solution (Table 2) [14], diluted to 1:10 with distilled water. It contains the necessary nutrients to support fungal growth and was diluted as in previous works to simulate the poor mineral conditions found in drained water from integral fuel tanks [4–6,15–21].

As our purpose was that only the seeded species developed, sterilisation of the nutrient solution was done in autoclave at

Table 2
Chemical composition (g/l) of the modified Bushnell–Haas nutrient solution [13]

Component	Concentration (g/l)
$MgSO_4 \cdot 7H_2O$	0.20
$CaCl_2$	0.02
KH_2PO_4	1.0
NH_4NO_3	1.0
60% $FeCl_3$ solution	2 drops
Distilled H_2O	Up to1 l

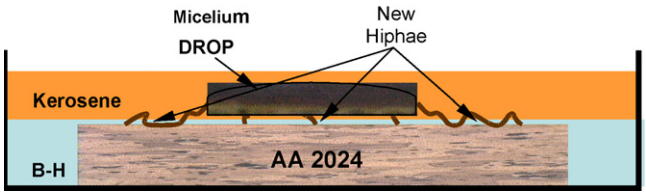

Fig. 1. Scheme of the "Drop test" showing fungal hyphae growth at the solution/fuel inter-phase while adhering to the alloy.

120 °C and 1.5 atm and all necessary tools in an oven at 110 °C. JP 1 fuel (kerosene) was used as only carbon source after being sterilised by filtration through a 0.45 μm porosity membrane to eliminate all spurious microbes.

Immediately after sterilisation, mycelium samples were introduced in 2 l separating funnels containing B–H diluted solution and jet A-1 kerosene in 10 to 1 aqueous solution/fuel volume rate. The fungus lied at the inter-phase and their spores developed after having been adapted to this two-phased system similar to its original habitat. Sowing was carried out in an air filtered, laminar flux cabin with sterilised tweezers and Pt hanza.

The aqueous phase, reflecting the composition change due to the fungal nutritional requirements for growing and including its metabolites, was used as electrolyte for polarisation. Two batch cultures were prepared in 2 l separatory funnels which aqueous phases were used as electrolytes after 60 and 400 days incubation at 30 °C.

2.4. Drop test

This is the fastest test to characterise the interaction between a metal and a microbe, reproducing the failure as it occurs in service. Its aim was analysing the mutual effect of fresh fungal biofilms growing on both metal surfaces [15–22].

During immersion in the cultures aqueous phase aggressiveness due to corrosive microbial growth take several weeks to affect a metal. On the contrary, the direct contact with the fungal mycelium hyphae reveals the most severe effect on the metal in much shorter periods because dilution is avoided [15–22].

The strain of *H. resinae* was enough corrosive to the alloy (or the alloy was so susceptible to MIC by the fungus), to reveal at the naked eye deep pitting after 5 days contact. The test consists in seeding a small piece of fungal mycelium over a 10 mm × 10 mm × 1 mm finely polished metallic surface (up to 0.25 μm diamond paste), in a Petri dish containing B–H 1:10 nutrient solution and kerosene as only carbon source, as shown in Fig. 1. As sterility respect to spurious microbes must be assured, but the alloy cannot be heated in autoclave because it might change its metallurgical state, it was sterilised by immersion in ethanol and then quickly evaporation by rapid pass over a burner flame.

During the drop test, the mineral nutrient B–H medium changes from innocuous at the beginning to very aggressive to the metal due to the fungal metabolism. Main factors are consumption of passivating nitrate ions (increasing the aggressive to passivating ions concentration rate) and also fuel degradation increasing the aqueous medium acidity.

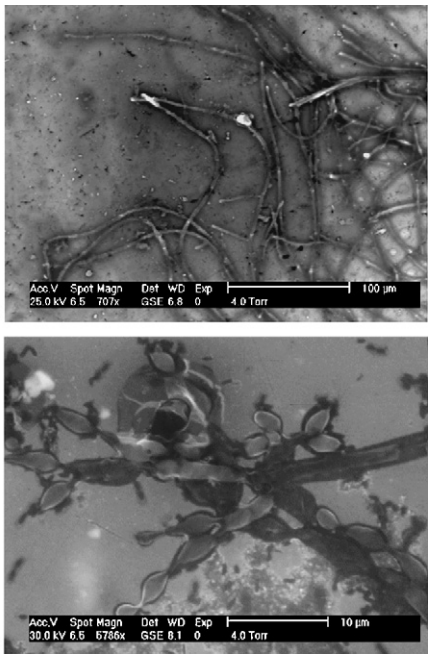

Figs. 2 and 3. ESEM aspect of *H. resinae* growing on rolled Al 99.999% and on AA2024 alloy 22 h aging.

Besides, previous works have demonstrated that *H. resinae* fungal mycelium may selectively up-take alloy elements from the metallic net which would be used as oligoelements [15–22]. Thus the fresh fungal biofilm morphology changes its aspect according to the necessary oligoelements available to the fungus in the metal as can be seen comparing Figs. 2 and 3. While the alloy underwent localised attack as shown in Figs. 4 and 5, the absence of any oligo metal determined the slow fungal growth on pure Al not producing any surface modification (Fig. 2), being

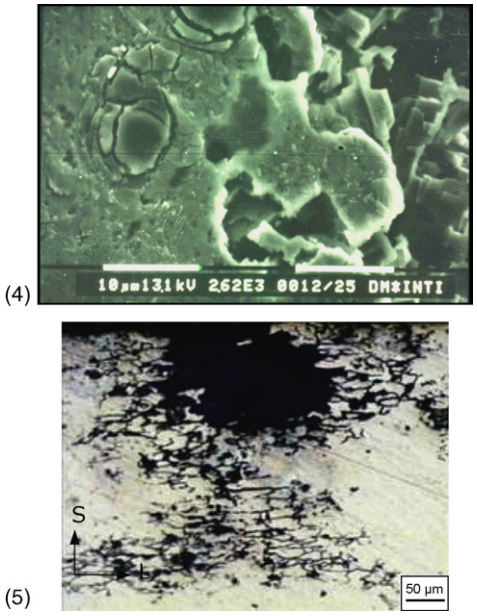

Figs. 4 and 5. SEM aspect in plan of the AA2024 T351 alloy and optical microscopy of cross-section after drop test under *H. resinae* fresh hyphae growing on it.

the aspect of the fresh growing fungal mycelium far from its characteristic aspect.

2.5. Electrochemical tests in the absence of fungal cultures

Potentiokinetic anodic polarisation of the AA2024 T351 alloy and of pure Al as reference were applied to investigate attack susceptibility. Samples of AA2024 T351 alloy and AA2024 in various ageing conditions, as well as two Al 99.999% thermo-mechanical conditions, were submitted to anodic polarisation using a LYP M-9 potentiostat at 60 mV/min scan rate. Measurements were performed at room temperature in a conventional Pyrex glass cell, through a Luggin capillary with a Pt counter electrode. Potential values were expressed respect to the saturated calomel electrode (SCE) used as reference in a three-electrode cell.

After polishing the metal samples, transparent epoxy resin curing in 10 min was used to prepare the working electrodes, leaving 1 cm^2 exposed area and establishing electric contact with a glass shielded copper wire. Silver paint was used in contacts.

The anodic curves were run in degassed solutions during 1 h bubbling with N_2 99.999%. Once the samples were immersed in the solution, their open circuit potential was left to evolve up to stable values. There followed anodic potential scanning from the attained E_c until surpassing 100 mV the pitting potential (E_p), at 60 mV/min scan rate.

After polarisation each sample was carefully dismantled and ultrasound cleaned with alcohol and acetone. Then, morphology-secondary phase analysis of the attack was performed through SEM with a Philips 515 coupled to an EDAX 9100.

Most of these analyses were performed in up to 10 replicates, having been obtained a very low dispersion. The corrosion rate differences observed were so evident for the distinct conditions that there was not need for pit density or deepness quantification. Corrosion rate increase was reflected in the pit size, deepness and morphology more than in their relative density.

3. Results

3.1. Drop test on the AA2024 alloy as compared to the Al 99.999% mycelium aspect

As can be seen in Figs. 2 and 3 the ESEM aspect of fresh fungal hyphae grew with very different aspect on both metals. Pure Al did not support the characteristic aspect of *H. resinae* through its usual vital signs (amount of growth, hyphal double wall and divisions, conidiophores, spores, etc.). AA2024 alloy produced different mycelium aspects according to different thermal treatments on the samples tested. The various treatments thus revealed the different surface availability of oligoelements that hyphae may up-take.

Accordingly, pure Al did not show any surface damage while the AA2024 T351 alloy underwent intense attack, as shown in Figs. 4 and 5 in plan and polished cross-section, respectively.

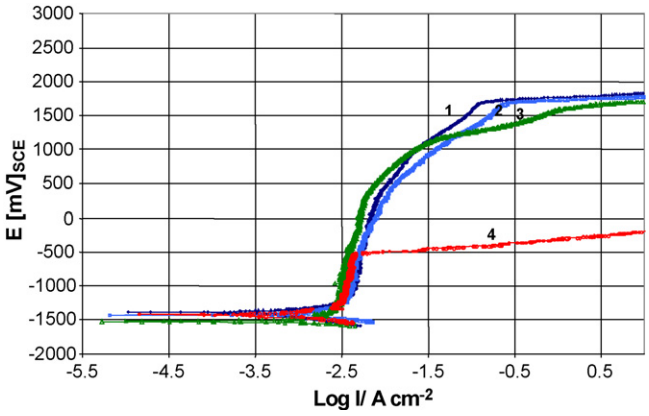

Fig. 6. Anodic polarization of Al 99.999% in deaereated media in mixtures of 0.1 M KNO_3 and (---1---) Non-Cl^-, (---2---) 5×10^{-4} M [Cl^-], (--3---) 0.02 M [Cl^-] and (---4---) 0.2 M [Cl^-]. (For interpretation of the references to colour in this figure legend, the reader is referred to the web version of the article.)

Previous findings [19–22] demonstrated that this could be due to the up-take capability of oligo-metals (Mg, Fe, Zn, etc.) by the growing hyphae as the MIC mechanism proposed for the alloy.

For different thermal treatments this paper shows that distinct elements could thus be extracted from the alloy correlative with diverse damage intensity and mycelium aspect, while there were none any available from Al 99.999%.

3.2. Pure aluminium

3.2.1. Anodic polarisation

Fig. 6 shows that the pitting potential (E_p) of pure Al evidences important decrease in 0.1 M KNO_3 solution for NaCl addition from 0.02 M concentration, while the passivity current and E_c did not depend on the aggressive Cl^- ion concentration.

Polarisation curves of pure rolled and recrystallised Al coincide and thus both metallurgical states would show the same behaviour before corrosion.

3.2.2. Morphology of the attack

SEM analysis of pure Al samples however, evidenced a different effect due to their thermo-mechanical conditions on size and shape of pits nucleated at E_p. Both micrograph sets evidenced the incidence in pits morphology, in the absence and in the presence of different Cl^- concentrations added to the 0.1 M KNO_3 solution, at the respective E_p.

Comparison of the results obtained for rolled and re-crystallised Al show that below a give threshold of aggressive Cl^- ions, both samples developed dissimilar hemispheric pitting. For rolled Al samples the pit bottom presented growing micro-pits while in re-crystallised pure Al typical polished hemispheric morphologies were observed. This difference might be related to higher density of dislocations of pure aluminium in the rolled over the re-crystallised state. In like manner, the effect of chloride ions seems to predominate over the difference in dislocation density given that in its presence the same morphology was found.

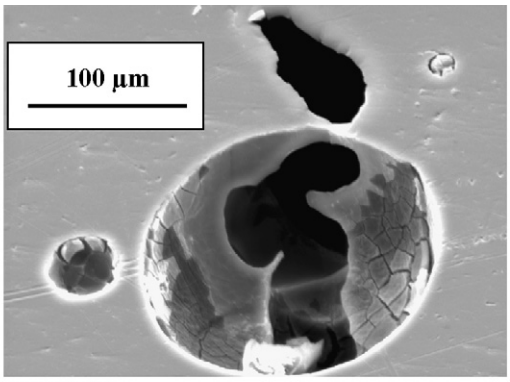

(7) 0.02M Cl

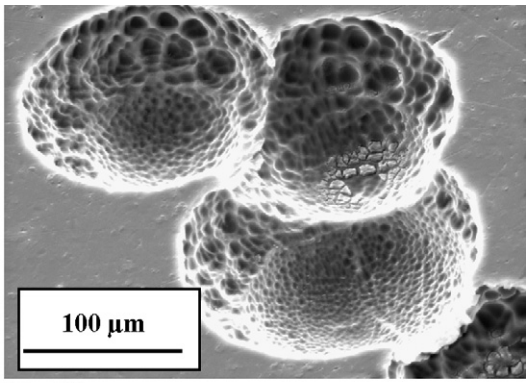

(8) Non Cl

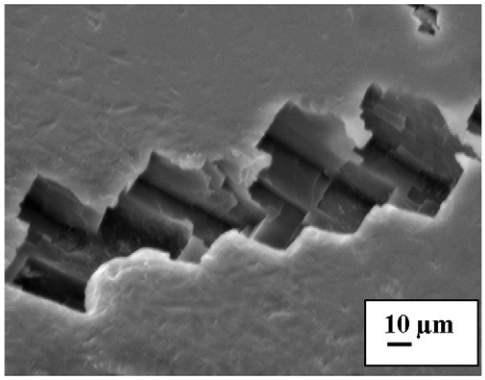

(9) 0.2M Cl $^-$

Figs. 7–9. Morphology of pits formed at E_p on rolled Al 99.999% in 0.1 M KNO_3 solution and different NaCl concentrations.

This study demonstrated an intermediate morphology existing between the hemispheric and fully crystallographic pitting attacks as the relation of aggressive to passivating ions concentration in the electrolyte increased. A great variety of pit shapes and sizes was observed, including pits propagating in hemispheric shape but having a crystallographic bottom. Likewise, strange cubic and rhomboid pits were observed, in accordance with Holt et al. [23]. These authors found that in the presence of Cl^- and $NO_3{}^-$ ions and in acid environments, triangular, rectangular and square pits formed following planes (1 1 1), (1 1 0) and (1 0 0).

Finally, by comparing polarisation curves from Fig. 6 with pitting morphologies in Figs. 7–9 for the rolled condition and Figs. 10–12 for the recrystallised one we may conclude that although at the E_p important changes are evident, only as starting from 0.02 M Cl^- concentration, intensity of the attack dramatically increased with a 10 times lower aggressive Cl^- ion aggregate. The dangerous tunnelling pit morphology generated was noticed for both pure Al conditions at the same compositions.

This effect of Cl^- ions above a well-defined threshold is especially relevant during the tests in fungal cultures because of the uncontrolled metabolic modification in the $NO_3{}^-/Cl^-$ rate, as demonstrated in synthetic solutions. Also in aircraft flying marine or coastal areas, where the aggressive Cl^- anion may reach high enough concentrations to promote tunnelling morphology, the fuel tank attack propagation should become much more intense.

3.2.3. Conclusions for pure Al tests simulating MIC in the absence of fungal cultures

- The E_c was affected neither by presence of aggressive ions nor by the material metallurgical state.
- Starting from 0.02 M, [Cl^-] increase showed significant metal E_p decrease.
- Polarisation curves were very similar for both metallurgical conditions.
- Intermediate morphology was found between fully hemispheric and fully crystallographic pitting attack.
- In the absence of chloride ions, none pit developed on rolled Al showed the typical polished bottom indicating the same corrosion rate propagation in all crystallographic orientations. Instead, micro-pits were always found on the pit walls.
- The presence of 0.02 M Cl^- ions promoted tunnel morphology dramatically increasing corrosion, through an important E_p decrease.

3.3. AA2024 T351 aluminium alloy

The AA2024 aluminium alloy is a thermo-treatable alloy of the 2xxx series, belonging to the duralumin group, widely used in the airspace industry due to its resistance to several types of damage. Common solutions like AA2024 T351 offer a combination of mechanical resistance, tenacity and resistance to fatigue very difficult to achieve by other alloys. However, its use does not limit to that industry, as it is also employed in manufacturing of gearing, axes, clockwork pieces, ammunition, coupling, etc.

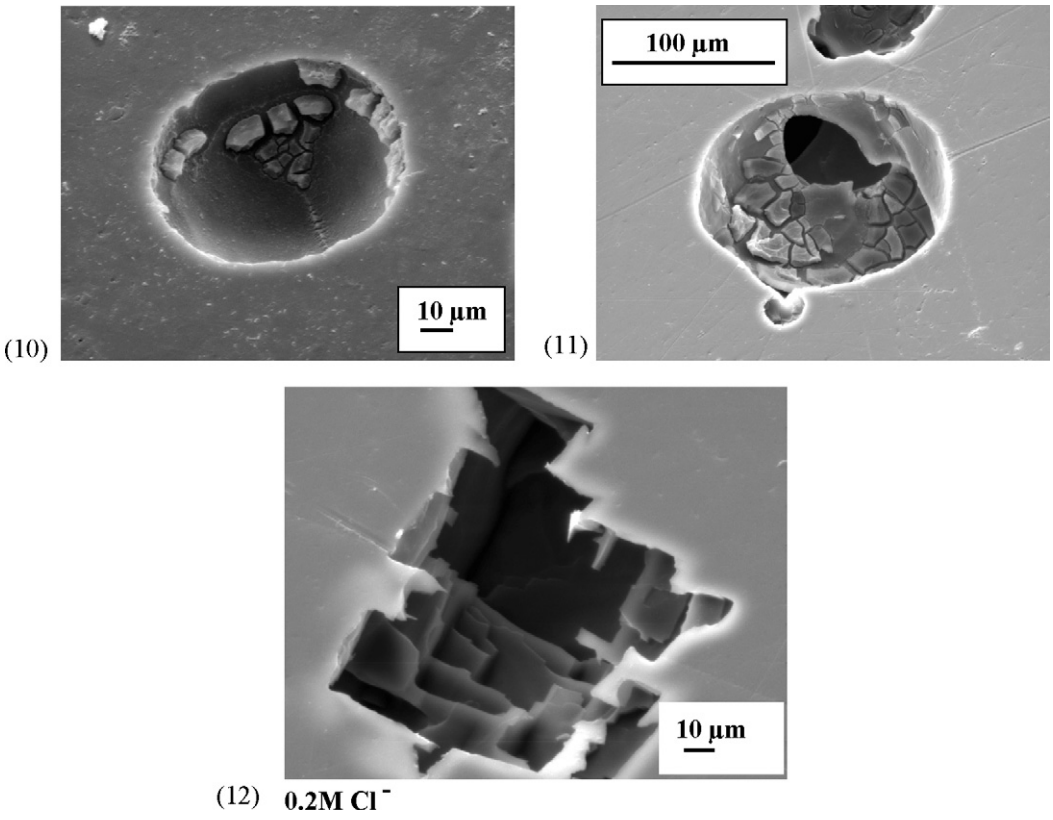

Figs. 10–12. Morphology of pits formed on recrystallised Al 99.999% in 0.1 M KNO_3 solution and different NaCl concentrations.

The main alloying elements are Cu and Mg, although it has a great variety of elements in too small quantities to be considered alloys and which, nevertheless, play an important role in its mechanical and corrosion resistance.

3.3.1. Experimental

Polished thermo-treated samples were assembled for electrochemical tests as in Section 2.5.

The electrolyte used was NH_4NO_3 10^{-3} M, deaereated since 1 h before polarisation, through N_2 99.99% bubbling to reveal the extensive passivity zone and to differentiate between E_p of the phases present in the alloy. This latter characterisation was performed through optical microscopy-EDX after polarisation.

3.3.2. Results and discussion

Comparing the anodic polarisation curves shown in Fig. 13 after different temperature and ageing times, a first peak of activity appears around 100 mVsce. It seems to correspond to E_p of the S phase (Al_2CuMg), according to EDX, active with respect to the matrix and to T4 treatment. Along the passivity zone different peaks appear corresponding to E_p of distinct phases of the alloy. The existence of two types of attack was noticed: on the precipitates and on the matrix. Polarisation revealed the most anodic or noble precipitates respect to the matrix, larger and more geometrically shaped (Al–Cu–Mn–Fe or type 1 phase precipitates), always remained damage-free. The 22-h aged alloy evidenced precipitates not only at grain boundaries but throughout the matrix, being their attack more extensive. This comparison also revealed that the 22-h aged alloy (maximum hardness) presents the highest activity, indicating its lowest corrosion resistance.

The matrix E_p is approximately 1990 mVsce, similar to that of pure Al in the absence of any aggressive ion, E_c coinciding for all metallurgical conditions tested.

As the alloy started becoming damaged, from 100 mVsce, this value should be considered its effective E_p bearing in mind that attacked zones might act as crack initiators facilitating subsequent propagation. Conversely, according to this work objective, it will provide higher security as the alloy was being studied to foresee aeronautical risks.

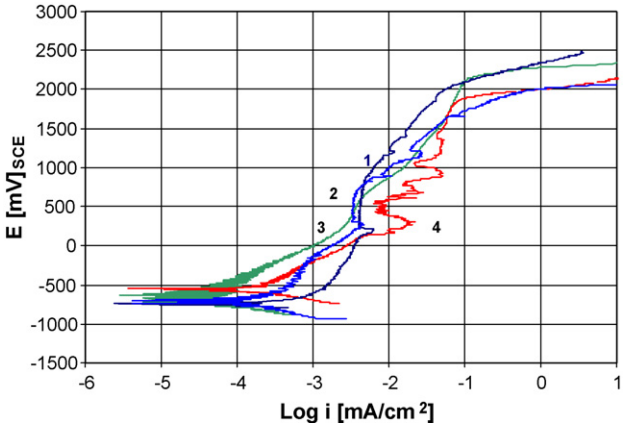

Fig. 13. Anodic behaviour of AA2024 alloy for different metallurgic conditions in deaereated 10^{-3} M NO_3NH_4: (---1---) aged 3 h, (---2---) aged 22 h (--3---) T351, (---4---) T4. (For interpretation of the references to colour in this figure legend, the reader is referred to the web version of the article.)

3.3.3. Conclusions on the AA2024 T351 alloy tests simulating MIC in the absence of fungal cultures

- The first peak of activity corresponded to E_p of the Al_2CuMg active precipitates (phase S) and should be considered as the alloy E_p.
- The alloy presenting higher hardness always showed major activity along the passive zone and higher distribution of the attack, as precipitation of the second phases occur not only at the grain boundaries but also within the grains.
- Type 1 precipitates (Al–Cu–Mn–Fe) always remained free of attack.
- The matrix E_p was similar to that of high purity Al in medium not containing aggressive species such as Cl^- ions.
- Pits were not wholly hemispheric but irregular shapes predominated.
- E_c did not change with the metallurgical state of the alloy.

4. Discussion

4.1. Electrochemical tests on AA2024 T351 alloy and on Al 99.999% in the fungal culture media

It is important to stress that sterility should be assured to study the effect of the *H. resinae* fungus avoiding MIC attack by any spurious ambient microbial contamination.

The electrolytes used were: (1) modified 1:10 B–H sterile solution, pH 5.5; and same solution inoculated with a strain of *H. resinae*, (2) after 60 and (3) 400 days incubation at 30 °C (pH was determined before each test); (4) also 0.1 M NaCl solutions were used to simulate high Cl^- concentrations that could be found in military aircraft tanks operating in coastal zones.

Cathodic runs were included in the presence of fungal cultures to show also their influence on this electrochemical result. Those curves were performed in oxygen-saturated solutions, through air bubbling, since 1 h previous to start and during each test, with constant magnetic stirring to maintain constant the hydrodynamic conditions of the system.

Typical anodic and cathodic results obtained on many replicates of AA2024 T351 alloy and on Al 99.999% in sterile and inoculated solutions are displayed in Figs. 14, 16 and 17.

The E_p of pure Al in the sterile mB–H solution used as support electrolyte was 2000 mVsce. When the anodic polarisation was performed in the same medium after 60 and 400 days incubation the drop in the KNO_3 concentration produced results as those shown in Fig. 14. E_p drop of the alloy was caused by its passivity decrease due to the metabolic consumption of N sources from the medium by the microbe. For the 60 days culture Fig. 14 shows the E_p drop to 60 mVsce and to −45 mVsce in the 400 days culture of fungus *H. resinae*. The 60 days B–H culture produced intermediate E_p being the morphology of attack also intermediate between those of the sterile and of 400 days culture media.

The lowest E_p was determined in 0.1 M NaCl solution. The electrochemical performance of AA2024 T351 alloy and Al 99.999% in medium of relatively high NaCl concentration showed that environmental conditions likely to occur in aircraft tanks operating in marine zones are extremely severe.

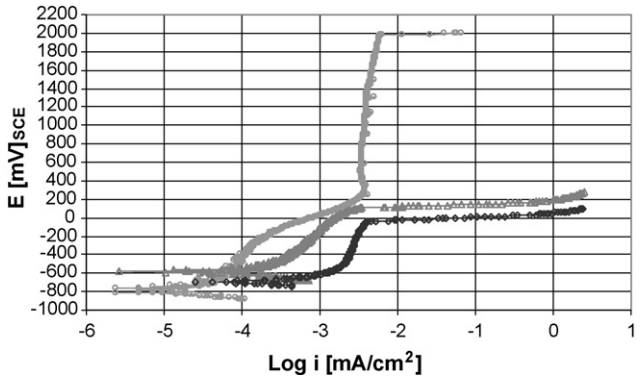

Fig. 14. Anodic polarisation of AA2024 T351 alloy in B–H 1:10 (---Δ---) sterile, 60 days and (---◊---) 400 days cultures deaereated. E_p = 2,000 mVsce, 60 mVsce and −45 mVsce, respectively.

Besides, if a probable synergy between Cl^- and MIC is taken into account, it is evident that the problem may bring about important corrosion damage to the aircraft structure.

The main anodic modification due to the fungal growth is due to the NO_3^- concentration decrease for an almost constant Cl^- concentration from the mB–H culture medium composition, on the basis of the E_p decrease with incubation time (Fig. 14). In this figure also the pH decay was included, that can be attributed to the fungal acidic metabolic degradation of fuel components (Fig. 15).

Also cathodic polarisation produced diverse electrochemical behaviour with incubation time in sterile and 400 days B–H solution culture, as can be appreciated for pure Al in Fig. 16. Analogous behaviour was shown by the AA2024 T351 alloy in the 60 and 400 days cultures. Cathodic polarisation evidenced that fungal proliferation significantly increases the limiting current of oxygen reduction (i_L) with incubation time, even quite longer after 60 days, when the fungus life cycle was overcome.

Fig. 17 shows the anodic and cathodic curves intersection, giving the corrosion potential, E_{corr} = −244 mVsce, and corrosion rate for the 400 days culture. As the real E_p is generally lower than the potentiokinetically obtained, this result shows that an alloy sample immersed in an aerated medium contaminated with the *H. resinae* is highly prone to suffer pitting damage.

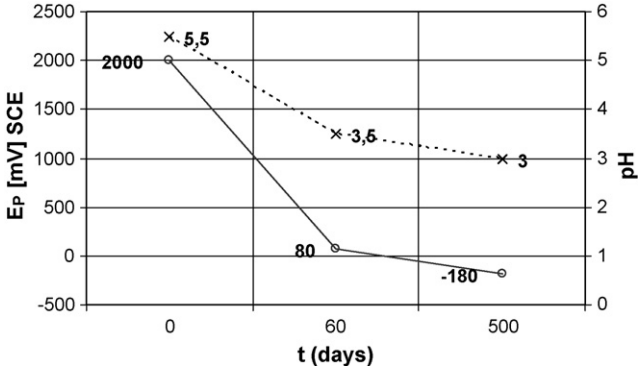

Fig. 15. E_p (---○---) of the AA2024 T351 alloy in the B–H 1:10 deaereated solution and pH (----×---) variation with incubation time.

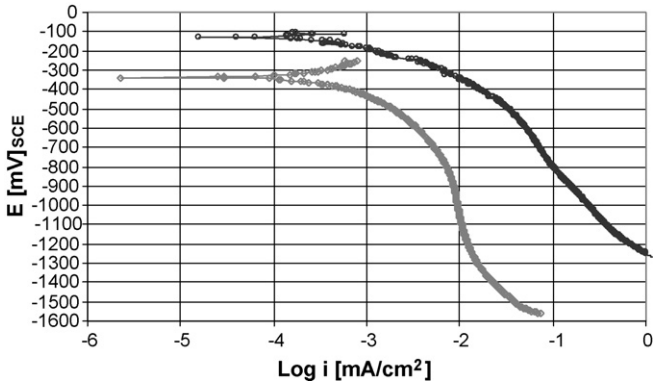

Fig. 16. Cathodic polarisation of rolled 99.999% Al in (---◊---) sterile and (---●---) in 400 days culture in O_2 saturated B–H 1:10 solution.

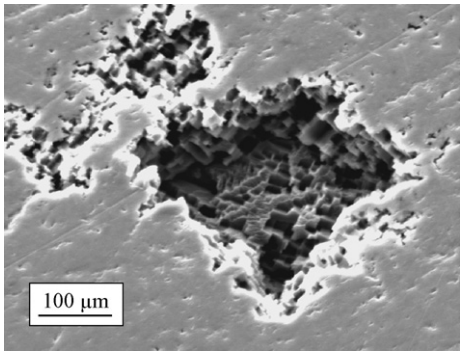

Fig. 18. SEM image of pits developed on rolled Al 99.999% after polarisation up to E_p in the 400 days culture in B–H 1:10.

Analysis of the polarisation results revealed striking E_p drop, booth for the AA2024 T351 (Fig. 14) and for pure aluminium, when comparing them in sterile and inoculated B–H media.

Even non-aggressive solutions as sterile B–H, produce lower E_p for the more susceptible alloy than for Al 99.999%. In this way, even through the anodic polarisation curves the existence of active zones selectively dissolving before reaching the matrix E_p evidences as highly risky any structural utilisation of the alloy without an appropriate protective coating.

4.2. Morphology characterisation after the different tests in the sterile medium as compared to its longest incubation culture

The anodic results exposed are in good agreement with the morphology observed in the metals submitted to polarisation up to surpassing the E_p in the distinct media.

Comparison between pitting SEM aspect of pure Al and of the respective alloy in the sterile nutrient solution evidences the higher susceptibility of the alloy, trough higher size pitting, even in the absence of fungal growth. These pits present well-defined geometric and hemispheric shapes similar to those in mixed solutions of KNO_3 and NaCl.

SEM aspect of the pitting morphology in plan and in cross-section of the rolled Al 99.999% in B–H 400-day culture is crystallographic, with highly localised current density inducing such extremely intense attack that differences in corrosion rate of distinct crystallographic plans seem to be negligible (Fig. 18).

The cross-section revealed in Fig. 19 the most dangerous tunnelling morphology in the most aggressive fungal culture. Besides the irregular pitting propagation deep tunnels are stress concentrating, the effect of which turns them extremely risky for aircraft fuel tanks. In the alloy those generalised pits propagate through grain boundaries. Conversely, risks dramatically decreases in sterile media because the pitting morphology does not propagate as tunnels.

A quick visual comparison of the much lower attack magnitude in the 60-day than in the 400-day culture evidenced its correlation to the increasing medium aggressiveness with the incubation time.

The results referred in the literature, according to which Cu precipitates as reduced deposits during the alloy attack were observed thorough SEM–EDX as globular deposits near the pits. EDX analyses resulted in the order of 30% of Cu and various high Cl. The alloy anodicaly polarised up to E_p in both most aggressive 400 days culture medium and in 0.1 M NaCl revealed important amount of Cu globular deposits, possibly resulting from the de-alloying mechanism proposed by Buchheit et al. [24].

Mixed hemispherical and crystallographic pitting of pure Al was observed through anodic polarisation up to E_p in 0.1 M NaCl solution, the most aggressive electrolyte tested.

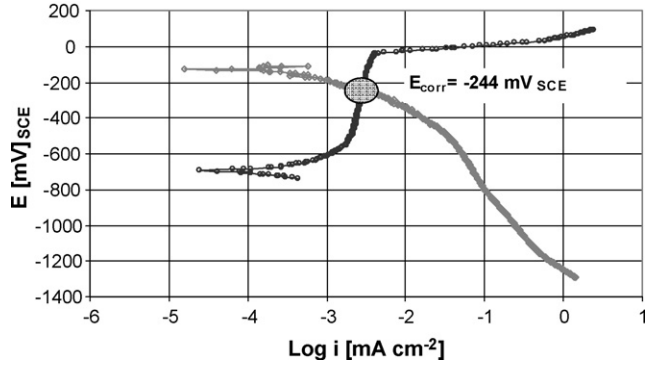

Fig. 17. Anodic and cathodic polarisation of the AA2024 T351 alloy in the 400 days culture in B–H 1:10; $E_p = -45$ mVsce, $E_{corr} = -244$ mVsce.

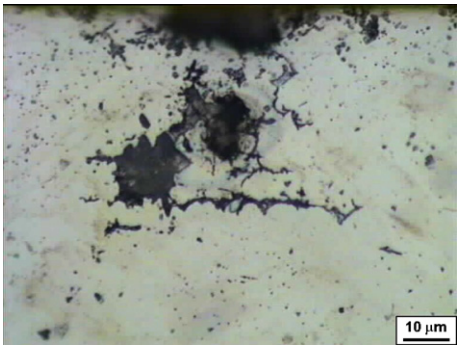

Fig. 19. Optical microscopy in cross-section of the same sample showing tunnelling structure propagation.

4.3. Microbial presence

The fungal growing mycelium morphology as well as the underlying metal aspect was evaluated through drop test on different thermo treated samples revealing, as shown in Figs. 2 and 3, the substratum effect on the fungal hyphae aspect. Also, as in Figs. 4 and 5, the reciprocal effect of the microbe attack on the metal damage was verified. The pure Al sample shown under the fungal biofilm in Fig. 2 did not produce, on the contrary, any surface alteration.

The environmental scanning electron microscopy (ESEM) aspects shown in Figs. 2 and 3 support previous findings, according to which MIC would be triggered by fungal metabolic needs [15,19–21], as also by other microbes [25], by selective metal ion extraction from metal and/or alloy networks [26].

Extra cellular polymeric material (EPM), mycelium in the case of fungi, and certain of its metabolites produced thus increase in the corrosiveness of an initially innocuous to an aggressive aqueous medium to a metal [27,28].

The 400 days incubation time included in this work, extremely longer than the mean fungal life cycle of around 60 days, allowed to demonstrate a new finding through the increased aggressiveness of the medium with incubation time, that the degradation products of the fungal mycelium autolysis also contribute to enhance a culture corrosiveness.

Previous MIC analyses were limited to the alive microbes (on up to 60 days cultures). However, in the case of military aircraft grounded during long periods, mycelium degradation process could occur in a tank. And, if the maintenance was not appropriately performed and the Air Base location is in a hot-humid climatic region, at subtropical-equatorial latitudes, such an aggressive situation could appear in fuel tanks.

4.4. Drop test

Research in progress show that the fungal mycelium proteinogram varied with the metal in which presence the biofilm was grown [15,19–22,26]. Through ESEM it was demonstrated that the fungus does not produce spores while growing on Al 99.999%. However, it produced different amount of spores and diverse biofilm morphology depending on the thermal treatment modifying the surface oligoelement availability of the AA2024 alloy on which it was seeded.

This would support the hypothesis that the surface "chemical sensing" capacity proposed for *H. resinae* [15,17–22,26] and other microbial species [4,21,22,24], could allow detection of oligo or harmful elements to their metabolism.

This biochemical capacity of microbial biofilms would provide a single mechanism explaining the metal ion up-take from a metal [20] or the protective barrier film formed on others [25].

The relevance of this research work lies in the new findings respect to MIC and in the very dangerous nature of the pitting morphology revealed. Major stress concentration in an aircraft wing during flight would produce catastrophic tunnel crack propagation.

5. Conclusions

(1) The E_p of the AA2024 T351 alloy more than that of the Al 99.999% dramatically decreases with the incubation time in mB–H solution inoculated with the fungus.
(2) All metal samples tested exhibited lowest E_p and tunnelling attack propagation in the most aggressive 0.1 M NaCl tested solution.
(3) The fungal proliferation produces important shift to higher cathodic limiting oxygen reduction with the incubation time.
(4) The alloy in over-aged condition always presented more active precipitates, selective dissolution and matrix pitting than in natural ageing condition.
(5) As the alloy E_c in the 400 days culture was higher than its E_p, pitting would spontaneously occur in a service contaminated fuel tank for similar conditions.
(6) The fungal mycelium autolysis contributed to the culture corrosiveness increase.
(7) The AA2024 T351 alloy showed extensive attack at grain boundaries and important Cu and Cl deposits in the 400-day culture.
(8) The most dangerous effect of MIC on the AA2024 T351 alloy is the tunnel morphology of pitting.

These conclusions demonstrate the MIC susceptibility of the AA2024 T351 alloy, the high risk of its use as lower skin of aircraft integral fuel tanks and the consequent need of an efficient protective coating.

The dangerous nature of the tunnel pitting morphology revealed would initiate catastrophic crack propagation during flight.

Acknowledgements

This work was financially supported by Contract EOARD (European Office of Aerospace Research and Development, Contracting Officer of USAF), No. F61775-01-WE080. The authors want to especially thank Dr. J. Galvele and Dr. R. Carranza for their helpful discussion of results. This work could not have been possible without the disinterested collaboration of the metallurgical and SEM staff of the CAC, Materials Department, CNEA.

References

[1] D.G. Parbery, Material und Organisem 6 (3) (1971) 161.
[2] W.A. Boggs. Lockheed-Georgia Co. Bulletin No. 680231, SAE Inc., 1968.
[3] J.A. Scott. National Air Transport Meeting, Atlanta, USA, 1971, Appendix III 363, p.1–7.
[4] M. Iannuzzi, B.M. Rosales, Proceedings of Materials Performance NACE, June 2003, pp. 62–66.
[5] B.M. Rosales, E.R. de Schiapparelli, Mater. Perform. 19 (8) (1980) 41–44.
[6] B.M. Rosales, E.R. de Schiapparelli, Proceedings of the 7th Int. Cong. Metallic Corrosion, Río de Janeiro, vol. 3, Brazil, 1978, pp. 1424–1430.
[7] E.S. Ayllón, B.M. Rosales, Corrosion, NACE 50 (8) (1994) 571.
[8] J.R. Galvele, S. de De Micheli, Corros. Sci. 10 (1970) 795.
[9] M. Ipohorsky. Publ. from the Institut of Tecnology Prof. J. Sabato 1995, (IT 38/95).

[10] Ch. Blanc, B. Lavelle, G. Mankowski, Aluminium Alloys (1996) 1559–1564.
[11] G.S. Frankel, J. Electrochem. Soc. 145 (6) (1998) 2285–2295.
[12] R.G. Buchheit, R.P. Grant, P.F. Hlava, B. Mckenzie, G.L. Zender, J. Electrochem. Soc. 144 (8) (1997) 2621–2628.
[13] Metals Handbook, Heat Treating of Aluminium Alloys, vol. 4, 9th ed., ASM, 1999, pp. 675–716.
[14] L.D. Bushnell, H.F.J. Haas, Bacteriol. 41 (1941) 653–673.
[15] B.M. Rosales, A. Puebla, D.S Cabral, Proceedings of the XI Int. Corrosion Congress 5B, Houston, USA, 1993, p. 3773.
[16] A.M. Palermo, S. Chichizola, B.M. Rosales, Proceedings of the Second Latin American Biodegradation and Biodeterioration Symposium, Gramado, Brasil, April 2–5, 1995.
[17] S. Chichizola, A.M. Palermo, B. Rosales, Proceedings of the 2nd NACE Latinoamerican Region Corrosion Congress, Paper 243, Río de Janeiro, 1996;
S. Chichizola, A.M. Palermo, B. Rosales, Proceedings of the 13th International Corrosion Conference, Paper 409, Melbourne, Australia, 1996.
[18] B. Rosales y, S. Chichizola, SAM'97 Meeting, Tandil, Argentina, 1997.
[19] R. Araya, B.M. Rosales, C. Bobadilla, R. Vera, Paper 780 Proceedings of the 15th International Corrosion Congress, Granada, Spain, 2002.
[20] R. Araya, B.M. Rosales, C. Bobadilla, R. Vera, Paper 177 Proceedings of the 5th NACE Latin-American Region Corrosion Congress, LATINCORR 2003, Santiago Chile, 2003.
[21] B.M. Rosales, Proceedings of the 5th NACE Latin-American Region Corrosion Congress LATINCORR 2003, Santiago, Chile, Plenary Lecture, 2003.
[22] B.M Rosales, M. Iannuzzi. Proceedings of the 5th NACE Latin-American Region Corrosion Congress, LATINCORR 2003, Santiago, Chile, 2003, Paper 243.
[23] R.T. Holt, M. Perry, J. Inst. Met. (1973) 101–151.
[24] R.G. Buchheit, M.A. Martinez, L.P. Montes, J. Electrochem. Soc. 147 (1) (2000) 119–124.
[25] B.M. Rosales, A.C. Cabezas, S.E. Chichizola, A. Fernández, Proceedings of the 3rd Latin American Biodegradation & Biodeterioration Symposium, Florianópolis, Brazil, 1998;
B.M. Rosales, A.C. Cabezas, S.E. Chichizola, A. Fernández, Proceedings of the 3rd NACE Latin American Region Corrosion Congress, Cancún, México, 1998.
[26] B. Rosales, R. Araya, C. Bobadilla, Proceedings of the 5th Latin American Biodeterioration and Biodegradation Symposium, Campeche, México, 28 March–1 April, 2004.
[27] J. Kruger, Uligh's Corrosion Handbook, 2000, Chap. 21, pp. 349–365.
[28] S.W. Borenstein, Microbiologically Influenced Corrosion Handbook, Industrial Press Inc., 1994.